Pflugers Arch - Eur J Physiol (2008) 457:197–209
DOI 10.1007/s00424-008-0496-3

SENSORY PHYSIOLOGY

Voltage-activated ion channels and Ca^{2+}-induced Ca^{2+} release shape Ca^{2+} signaling in Merkel cells

Rebecca Piskorowski · Henry Haeberle · Mayuri V. Panditrao · Ellen A. Lumpkin

Received: 23 December 2007 / Revised: 3 March 2008 / Accepted: 13 March 2008 / Published online: 16 April 2008

Abstract Ca^{2+} signaling and neurotransmission modulate touch-evoked responses in Merkel cell–neurite complexes. To identify mechanisms governing these processes, we analyzed voltage-activated ion channels and Ca^{2+} signaling in purified Merkel cells. Merkel cells in the intact skin were specifically labeled by antibodies against voltage-activated Ca^{2+} channels ($Ca_V2.1$) and voltage- and Ca^{2+}-activated K^+ (BK_{Ca}) channels. Voltage-clamp recordings revealed small Ca^{2+} currents, which produced Ca^{2+} transients that were amplified sevenfold by Ca^{2+}-induced Ca^{2+} release. Merkel cells' voltage-activated K^+ currents were carried predominantly by BK_{Ca} channels with inactivating and non-inactivating components. Thus, Merkel cells, like hair cells, have functionally diverse BK_{Ca} channels. Finally, blocking K^+ channels increased response magnitude and dramatically shortened Ca^{2+} transients evoked by mechanical stimulation. Together, these results demonstrate that Ca^{2+} signaling in Merkel cells is governed by the interplay of plasma membrane Ca^{2+} channels, store release and K^+ channels, and they identify specific signaling mechanisms that may control touch sensitivity.

Keywords Merkel · Mechanotransduction · Touch · BK · Ion channel · Ca^{2+} · CICR

Abbreviations

CICR	Ca^{2+}-induced Ca^{2+} release
IBTX	Iberiotoxin
TG	Thapsigargin

R. Piskorowski · M. V. Panditrao
Department of Physiology,
University of California, San Francisco,
600 16th Street,
San Francisco, CA 94143, USA

H. Haeberle
Neuroscience Graduate Program,
University of California,
San Francisco, CA 94158-2324, USA

H. Haeberle
Department of Neuroscience, Baylor College of Medicine,
One Baylor Plaza,
Houston, TX 77030, USA

E. A. Lumpkin (✉)
Department of Neuroscience, Molecular Physiology and Biophysics, and Molecular and Human Genetics,
Baylor College of Medicine,
One Baylor Plaza, Smith Building, room S636A,
Mail stop BCM295,
Houston, TX 77030, USA
e-mail: lumpkin@bcm.edu

Introduction

The signaling cascades that govern sensory transduction in vertebrate touch receptors are largely unknown; however, Ca^{2+} signaling seems to be necessary for touch-evoked activity in at least one subtype, the slowly adapting type I (SAI) receptor. They are one of the four major subtypes of touch receptors in primate fingertips and are critical for distinguishing the form of objects and fine textures [1]. SAI receptors, which comprise epidermal Merkel cells and somatosensory afferent terminals [2, 3], are concentrated in areas of the skin that are highly touch-sensitive, including whisker follicles, fingertips, and touch domes (reviewed in [4]).

Studies using semi-intact preparations have implicated Ca^{2+} signaling in SAI responses. For example, inorganic antagonists of Ca^{2+} channels dramatically inhibit SAI responses [5, 6]. Moreover, drugs that enhance Ca^{2+} release from intracellular stores, such as caffeine and 1 μM ryanodine, were found to increase slowly adapting responses whereas procaine, a Ca^{2+}-induced Ca^{2+} release (CICR) inhibitor, diminished these responses [7]. One important limitation of these semi-intact recordings is that they cannot reveal the site of Ca^{2+} action because touch-evoked activity is monitored by measuring action potentials, which are downstream of sensory transduction. Thus, it is unclear whether the Ca^{2+} signaling critical for touch responses occurs in the Merkel cell, the neuron or both.

Several lines of evidence indicate that Merkel cells have Ca^{2+} signaling pathways that might be activated during touch. First, voltage-activated Ca^{2+} currents have been recorded from rat footpad Merkel cells [8]. Second, mouse Merkel cells show robust increases in intracellular free Ca^{2+} concentration ($[Ca^{2+}]_{in}$) upon depolarization that require the activity of L-type and P/Q-type Ca^{2+} channels [9]. Consistent with these results, Merkel cells express transcripts encoding L-type ($Ca_V1.2$), P/Q-type ($Ca_V2.1$) and N-type ($Ca_V2.2$) voltage-activated Ca^{2+} channels [9]. Third, Merkel cells express two isoforms of store release channels, inositol-(1,4,5)-triphosphate receptors (IP_3R) type I and II [10]. Fourth, Merkel cells express espins [11], Ca^{2+}-resistant cytoskeletal regulatory proteins that are found in sensory and neuronal cell types that have large Ca^{2+} transients, including Purkinje cells [12] and retinal Müller cells [13]. Finally, mechanical stimuli, such as hypotonic-evoked cell swelling, elicits cytoplasmic Ca^{2+} increases in Merkel cells [14–16].

To functionally characterize cellular mechanisms that shape Ca^{2+} signaling in Merkel cells, we have used Ca^{2+} imaging and whole-cell voltage-clamp recordings to directly record from pure populations of GFP-expressing Merkel cells dissociated from the skin of transgenic mice. We find that the Merkel cell's membrane potential is governed by voltage-activated Ca^{2+} channels as well as multiple voltage-activated K^+ channels, including the large-conductance voltage- and Ca^{2+}-activated K^+ channel (BK_{Ca} channel). These results are bolstered by the detection of both $Ca_V2.1$ and BK_{Ca} channels with immunohistochemistry and the amplification of transcripts encoding the pore-forming α subunit of BK_{Ca} channels (KCNMA1) as well as multiple β subunits of this channel (KCNMB1, KCNMB2, and KCNMB4). Moreover, we show that the interplay of voltage-activated Ca^{2+} channels, Ca^{2+} release from intracellular stores and voltage-activated K^+ channels govern the extent and time course of Ca^{2+} signaling in Merkel cells activated by cell swelling.

Materials and methods

Animal use

Experiments were performed with Merkel cells from *Math1*-nGFP transgenic mice [17], which express nuclear-localized GFP driven by *Math1* enhancer sequences. In these mice, GFP is expressed in Merkel cells but not in other skin cells [17]; therefore, we used GFP fluorescence to identify Merkel cells in skin sections and in isolated epidermal cells. Use of experimental animals was approved by the Institutional Animal Care and Use Committees of University of California, San Francisco and Baylor College of Medicine.

Immunohistochemistry

Juvenile mice (P15–P21) were used for histological analysis because touch-dome density at this age is higher than in adult mice, which greatly facilitated analysis of touch-dome Merkel cells in skin cryosections. Although dissociated-cell experiments required neonatal mice (see below), older animals were used for histological analysis because the firing rates of touch-evoked responses are not fully mature in neonates [18]. It is possible that protein expression changes in Merkel cells during this developmental period; however, as detailed below, our functional results from neonatal Merkel cells are entirely consistent with our histological results from juvenile mice. Moreover, SAI response thresholds, receptive field sizes, and firing patterns are remarkably similar in neonatal and adult mice [3].

Juvenile mice were euthanized by CO_2 inhalation. The whisker pads and dorsal skin were shaved with animal clippers and de-haired with a depilatory cream (Surgicreme). Skin was dissected and fixed in cold 4% paraformaldehyde for 30 min. After rinsing with phosphate-buffered saline (PBS), tissue was cryoprotected for 12 h at 4°C in a solution containing two parts OCT (Tissue-Tek) and one part 20% sucrose. Tissue was frozen in OCT and cryosectioned into 12–16 μm sections orthogonal to the plane of the skin. Sections were blocked overnight at 4°C in PBS supplemented with 0.1% tritonX-100 (PBST) and 5% normal goat serum (NGS). Primary antibodies were diluted in PBST supplemented with 1% NGS and incubated for ~4 h at room temperature. The anti-BK_{Ca} antibody (Alomone labs) was diluted 1:450, and the anti-$Ca_V2.1$ antibody (Chemicon) was diluted 1:200. Goat anti-rabbit, Alexa-594 conjugated, secondary antibodies (Molecular Probes) were diluted 1:1,000 in PBST and incubated for 30 min at room temperature. Confocal images were taken on an upright confocal microscope equipped with a 63X, 1.4NA objective

lens (Pascal, Carl Zeiss). Pinholes were set such that optical sections were ≤1.5 μm; individual optical sections are shown. Images were prepared for publication in Photoshop (version CS, Adobe).

Cell preparation

To isolate a sufficient number of Merkel cells for in vitro analysis, we dissociated epidermal cells from neonatal mice prior to the first hair cycle (P1–P8). In older animals, epidermal cells are more difficult to dissociate and Merkel-cell yields were too low to allow functional experiments. *Math1*-nGFP mice were euthanized by decapitation with sharp scissors. The skin from the body and face was dissected and washed in 10% hibiclens and Hanks buffered salt solution (HBSS) supplemented with penicillin, streptomycin, and fungizone. Typically, tissue from whisker pads and touch domes was pooled to ensure an adequate number of Merkel cells for electrophysiological recordings; when noted, however, Merkel cells were isolated only from touch domes. Tissue was cut into strips (1×0.2 cm) and incubated for 1 h at room temperature in dispase (25 $U \cdot ml^{-1}$; BD Biosciences) in Ca^{2+}- and Mg^{2+}-free HBSS. The epidermis was peeled from the dermis with sharp forceps and incubated at 37°C in 0.05–0.1% trypsin and 1 mM EDTA-4Na solution (Gibco) for 15 min with periodic vortexing. Trypsin was neutralized with fetal bovine serum (FBS) and the cells were filtered with 70- and 40-μm cell strainers, spun at 400×*g* for 11 min then resuspended in SMEM with 10% FBS. GFP-positive Merkel cells were purified from the epidermal-cell suspension by fluorescence-activated cell sorting (FACS; FACSAria, BD Biosciences; [9]). Merkel cells were plated onto collagen-coated coverslips and grown in 5% CO_2 at 37°C in serum- and antibiotic-free keratinocyte media (CNT-02, Chemicon).

Reverse transcription and polymerase chain reaction

GFP-positive Merkel cells were purified from P1–P5 mice using FACS with strict gating conditions to achieve ≥95% purity. Total RNA from 4×10^4 GFP^+ cells was isolated using commercially available reagents (Qiagen RNeasy kit) and DNAse-treated according to manufacturer's instructions to remove contaminating genomic DNA. First-strand cDNA was synthesized using $oligo(dT)_{12–18}$ primers at 42°C for 2 h using SuperScriptII (Invitrogen). PCR products were amplified with touchdown PCR using a PTC-200 Peltier thermal cycler (MJ Research); cDNA from ~500 cells was used for each PCR. In all experiments, control PCRs lacking cDNA template were performed to confirm the absence of contamination, and primer performance was verified with brain cDNA. To ensure that amplicons were not derived from genomic DNA, primers were designed to span introns. Primer pairs, which were designed with Primer3 [19], included: BK_{Ca} α subunit/KCNMA1 (forward: GGGTCAACATT CCCATCATC, reverse: CAACCACCATCCCCTAAGTC, predicted product: 367 bp), β1/KCNMB1 (forward: CTGGGAGTGGCAATGGTAGT, reverse: TGGATAGG ACCTGTTGAGC, predicted product: 502 bp), β2/KCNMB2 (forward: CAGAGCGTGTGGACAGAAGA, reverse: TTGATCCGTTGGATCCTCTC, predicted product: 479 bp), β3/KCNMB3 (forward: TGTCCAAAT CACGCTACAGG, reverse: CGAGTGGCTCAGGTTT ACGA, predicted product: 361 bp), β4/KCNMB4 (forward: CTTCATCTTCGGCTTCTGCT, reverse: AGGACCAC GATGAGAACACC, predicted product: 474 bp). KCMNB1 primer pairs yielded multiple products of different sizes; therefore, amplicons were cloned and sequenced to confirm the transcripts' identities.

Live-cell imaging

After two days in culture, Merkel cells were loaded for 20 min with 2 μM fura-2 acetoxymethyl ester (Molecular Probes) in a modified Ringer's containing (in mM): 110 NaCl, 5 KCl, 10 HEPES (pH 7.4), 10 D-Glucose, 2 $MgCl_2$, 2 $CaCl_2$, and 30 mM mannitol (osmolality: 290 $mmol \cdot kg^{-1}$). Cells were allowed to digest the ester bonds for 30 min and were imaged in Ringer's solution. Twenty percent hypotonic solutions (232 $mmol \cdot kg^{-1}$) were formulated like the loading Ringer's solution, except that they lacked 30 mM mannitol. Merkel cells were depolarized with high-K^+ Ringer's solution containing (in mM): 5 NaCl, 135 KCl, 10 HEPES (pH 7.4), 10 D-glucose, 2 $MgCl_2$, and 2 $CaCl_2$. Data were acquired with Metafluor software of Meta Imaging series (version 6.4.7, Molecular Devices), and analyzed with custom programs written in Igor Pro (version 5.03, Wavemetrics). Because Ca^{2+} signals during sustained hypotonic stimulation decayed only slightly in the absence of tetraethylammonium (TEA), decay times were defined as the elapsed time from 100% to 80% of the peak fura-2 ratio.

Electrophysiology

Currents were recorded from Merkel cells after 1–5 days in culture with an Axopatch 200B amplifier, a Digidata 1322A interface and a personal computer running pClamp software (Axon Instruments). Pipettes were pulled from borosilicate capillary glass (World Precision Instruments) with a Flaming/Brown micropipette puller (model P-97; Sutter Instruments). Pipette resistance ranged from 0.9–2.0 MΩ. Pipette tips were coated with beeswax to reduce pipette capacitance. The perforated patch technique was used for

all whole-cell recordings to preserve endogenous Ca^{2+} buffers [20]. To prevent amphotericin B from entering the bath prior to seal formation, pipette tips were filled with internal solution and the backs of pipettes were filled with internal solution supplemented with 20 μM amphotericin B. After a giga-ohm seal was established, the series resistance decreased to 10–20 MΩ within 5–10 min. The membrane capacitance, which was typically between 25–40 pF, was measured from the decay constant during a 20 ms voltage step with pClamp. Capacity current was then removed using the amplifier circuitry, and series resistance compensation was set at 80–95%. For pulled-patch recordings, no series resistance compensation was performed, as series resistance was generally <5 MΩ. Signals were filtered at 5 kHz and digitized at 25 μs. Leak currents were subtracted during whole-cell recordings with a P/4 protocol.

Potassium currents in the whole-cell configuration were recorded in extracellular Ringer's solution. The pipette solution contained (in mM): 70 KOH, 70 KCl, 10 NaCl, 1 $MgCl_2$, 0.5 $CaCl_2$, 5 EGTA, 2 MgATP, and 10 HEPES (pH 7.2). The internal solution contained approximately 100 nM internal Ca^{2+} as estimated by emission of fura-2 fluorescence at 340 and 380 nm. Iberiotoxin (IBTX; Tocris, Ellisville, MO, USA) was dissolved in Ringer's solution at 100 nM and perfused into the recording chamber. Block of IBTX-sensitive currents typically took at least 10 min to reach steady state; during this time the series resistance was closely monitored. For inside-out patch recording, the extracellular (pipette) solution contained 155 NaCl, 5.8 KCl, 0.9 $MgCl_2$, 1.3 $CaCl_2$, 0.7 NaH_2PO_4, 5.6 Glucose, and 10 HEPES (pH 7.4). The internal (bath) solution was composed of three different solutions comprising (in mM): 70 K-Gluconate, 70 KCl, 10 NaCl, 1 $MgCl_2$, and 10 HEPES (pH 7.2), with differing concentrations of Ca^{2+} and EGTA to attain subnanomolar, 2 μM or 10 mM $[Ca^{2+}]_{free}$. For each solution, initial $[Ca^{2+}]$ and EGTA concentrations were based on estimates from MaxChelator (http://www.stanford.edu~cpatton/maxc.html/). The $[Ca^{2+}]_{free}$ of each solution was measured with fura-2 fluorescence and adjusted as needed.

For recording voltage-activated Ca^{2+} currents in whole-cell configuration, the pipette solution contained: 70 CsOH, 70 CsCl, 10 NaHEPES, 2 $MgCl_2$, 0.44 $CaCl_2$, 2 EGTA, 3 Mg-ATP, pH 7.2. The external solution with Ba^{2+} as the charge carrier contained: 104 NaCl, 5 KCl, 1 $MgCl_2$, 25 $BaCl_2$, 30 TEACl, 10 Glucose, and 10 HEPES (pH 7.4). The external solution with Ca^{2+} as the charge carrier contained: 104 NaCl, 5 KCl, 1 $MgCl_2$, 25 $CaCl_2$, 30 TEACl, 10 Glucose, and 10 HEPES (pH 7.4). The external solution with reduced Cl^- contained: 104 Na-Gluconate, 5 KCl, 2 $MgCl_2$, 2 $CaCl_2$, 25 $BaCl_2$, 30 TEACl, 10 Glucose, and 10 HEPES (pH 7.4). Junction potentials between the external Ba^{2+} solution and the reduced Cl^- solution were measured using a flowing 3 M KCl bridge as described [21]. The reduced Cl^- external solution had an offset of −9.4 mV that was corrected. Electrophysiology data were analyzed with Igor Pro (version 5, Wavemetrics). Errors are expressed as standard errors of the mean (SEM).

Results

Merkel cells express voltage-activated Ca^{2+} channels

Previous experiments demonstrated that purified Merkel cells express transcripts encoding voltage-activated Ca^{2+} channels [9]. To determine whether Merkel cells express these ion-channel proteins in the intact skin, we used immunohistochemistry. Merkel cells in touch domes and in whisker follicles robustly label with an antibody against $Ca_V2.1$, a P/Q-type Ca^{2+} channel (Fig. 1a–c). We observed a striking staining pattern in touch-dome Merkel cells: $Ca_V2.1$ was expressed on the cell surface with obvious staining in microvilli, as well as in intracellular puncta (Fig. 1b,c). By contrast, Merkel cells in whisker follicles displayed a more punctate immunoreactivity (Fig. 1a). Antibodies recognizing the N-type isoform $Ca_V2.2$ and the L-type isoform $Ca_V1.2$ showed only weak immunoreactivity in Merkel cells that was often indistinguishable from non-specific labeling (data not shown). It is interesting to note that $Ca_V1.2$ immunoreactivity in whisker follicles was consistently observed in the somatosensory afferents that contacted Merkel cells.

To characterize currents through voltage-activated Ca^{2+} channels, we dissociated Merkel cells from whisker pads and touch domes and recorded from these cells in the whole-cell voltage-clamp configuration with perforated-patch techniques. Membrane currents were recorded in response to 50-ms voltage steps from −80 mV to +90 mV (Fig. 1d). To prevent current carried by voltage-activated Ca^{2+} channels from being masked by K^+ current (see below), we replaced K^+ in the pipette with Cs^+ and included 30 mM TEA in the external solution. Under these conditions, about half of the Merkel cells (14/30) had detectable inward currents through voltage-activated Ca^{2+} channels (Fig. 1d). In external Ba^{2+} solutions, these currents began to activate at −20 mV, with a peak inward current at +10 mV of 35±28 pA, or −1.7±0.2 pA/pF (N=14 cells; Fig. 1e,f). For those cells with a peak Ba^{2+} current greater than 50 pA, we also recorded currents in external 25 mM Ca^{2+} solutions. These currents began to activate at +10 mV and reached maximal activation at +30 mV of 30±18 pA, or −1.4±0.3 pA/pF (N=4 cells; Fig. 1e,f).

In most Merkel cells (85%), Cl^- carried a current of varying magnitude. In solutions with 25 mM external Ba^{2+}, the Cl^- current ranged from 0–200 pA at +90 mV

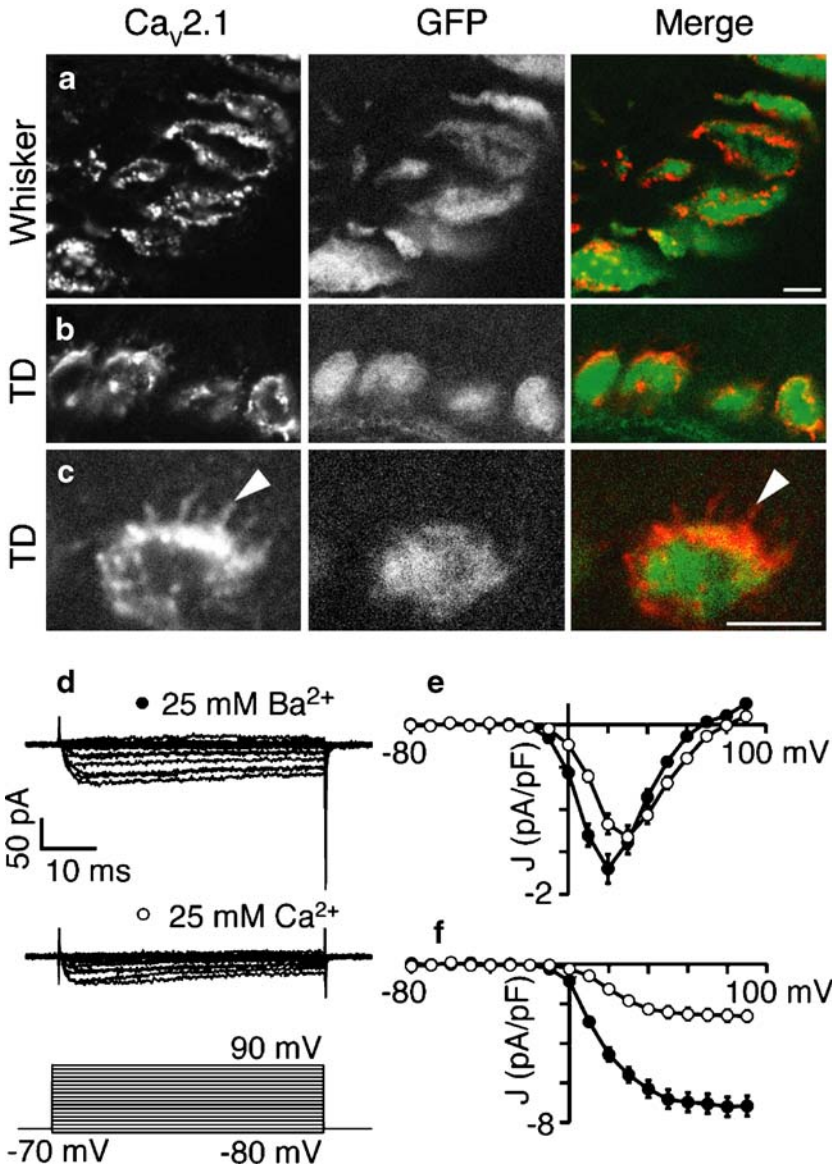

Fig. 1 Merkel cells express voltage-activated Ca^{2+} channels. $Ca_V2.1$ expression was detected by antibody staining in GFP^+ Merkel cells in whisker follicles (**a**) and touch domes (**b–c**). Immunoreactivity was detectable in cell somata and microvilli (*arrowhead*). *Right panels* show merged images of immunoreactivity (*left panels* and *red*) and GFP fluorescence (*middle panels* and *green*). The *scale bar* in **a** applies also to **b**; all *scale bars* represent 10 μm. **d** Representative whole-cell Ba^{2+} (*top*) and Ca^{2+} (*middle*) currents recorded from a Merkel cell in response to a series of depolarizing steps (*bottom*). **e** Peak Ba^{2+} (*filled circles*) and Ca^{2+} (*open circles*) current densities during the depolarizing step plotted as a function of membrane potential. **f** Peak Ba^{2+} (*filled circles*) and Ca^{2+} (*open circles*) tail current densities at the −70 mV step plotted as a function of the preceding depolarizing step. For both **e** and **f**, (N=14 cells for Ba^{2+} and N=4 cells for Ca^{2+}). *Error bars* denote SEM

with a mean of 44±35 pA, or 2.0±0.3 pA/pF (N=11 cells, Fig. 2a,b). In Ringer's solutions with 2 mM external Ca^{2+} and 6 mM external TEA to block voltage-activated K^+ currents, the observed outward current was larger, with a mean current at +90 mV of 159±54 pA or 5.0±0.5 pA/pF (N=8 cells; Fig. 5d,h). This outward current frequently masked Ca^{2+}-channel currents. To determine whether Cl^- carried this current, the reversal potential was measured with an instantaneous current–voltage protocol (Fig. 2c,d) before and after reducing the external Cl^- concentration. From the Goldman–Hodgkin–Katz voltage equation [22], decreasing $[Cl^-]_{out}$ while leaving the concentrations of all other internal and external permeable ions unaltered will shift the reversal potential to more positive voltages, as we observed (Fig. 2d). If the current was carried by permeant cations rather than Cl^-, then a shift in the reversal potential would not be expected under these conditions.

The small magnitude of the Ca^{2+} channel currents and the varying level of Cl^- current prevented a detailed pharmacological characterization of the Merkel cell's Ca^{2+} channels. Nonetheless, the permeation properties, deactivation kinetics and activation range of voltages, as measured by the tail current at steady state (Fig. 1f), is consistent with those of P/Q and L-type voltage-activated Ca^{2+} channels [23], which are necessary for depolarization-induced Ca^{2+} transients in dissociated Merkel cells [9].

Merkel cells have CICR from internal Ca^{2+} stores

Although voltage-activated Ca^{2+} currents are quite small in cultured Merkel cells (Fig. 1d–f), depolarization-induced Ca^{2+} transients are robust (Fig. 3 and [9]). We therefore asked whether Ca^{2+} release from internal stores contributes to these responses. To characterize Ca^{2+} stores in Merkel

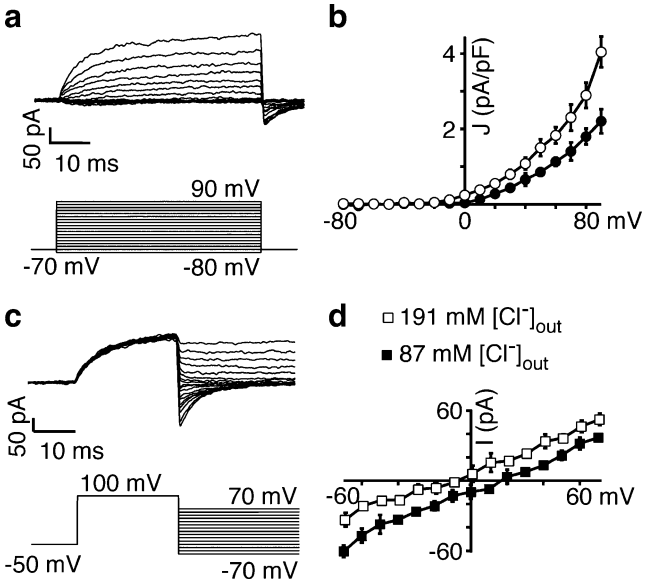

Fig. 2 Merkel cells express a Cl^- conducting current. A majority of the Merkel cells recorded with intracellular Cs^+ solution and 25 mM external Ba^{2+} had voltage-dependent currents (**a**, *top panel*) that activated in response to a series of voltage steps (**a**, *lower panel*). **b** Steady-state current densities with either 25 mM external Ba^{2+} (*filled circles*) or 25 mM external Ca^{2+} (*open circles*) are plotted as a function of voltage (N=11 for Ba^{2+} and N=4 for Ca^{2+}). **c** To identify the permeant ion, instantaneous current–voltage curves were collected (*upper panel*) with the tail-current voltage protocol shown (*lower panel*). **d** To estimate reversal potentials, current–voltage relations were measured before (*open squares*) and after (*filled squares*) reducing the external [Cl^-] from 191 to 87 mM (N=4, *error bars* denote SEM). Gluconate was substituted for Cl^- to maintain isotonicity

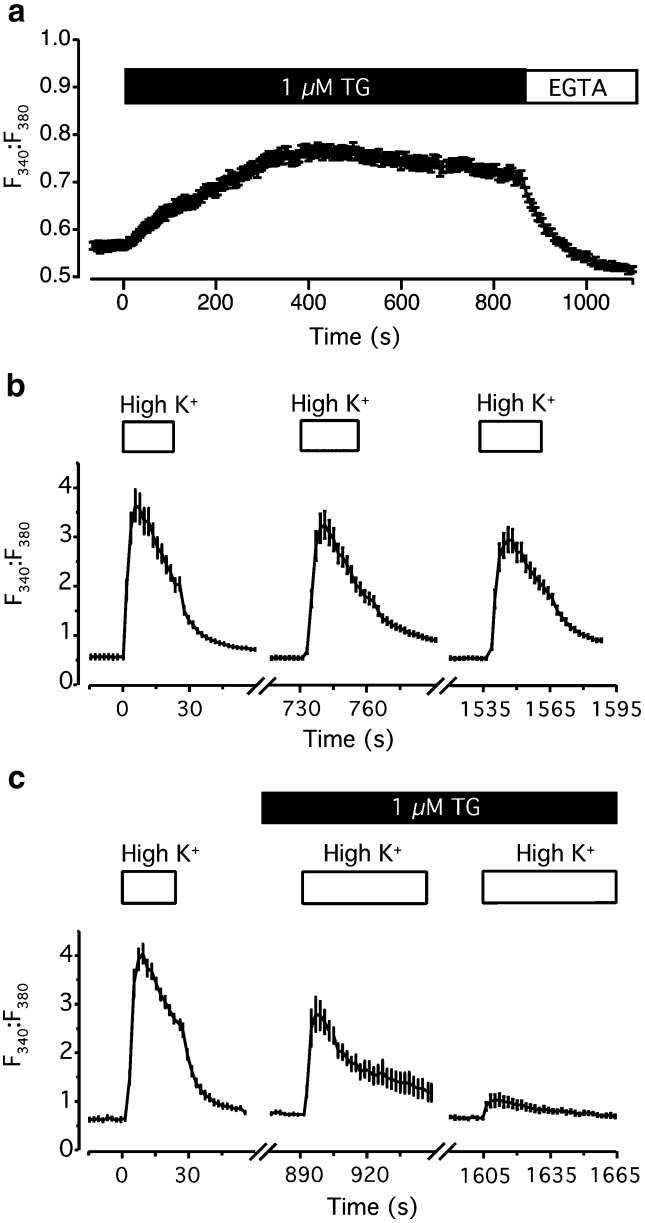

Fig. 3 Internal Ca^{2+} stores contribute to depolarization-evoked Ca^{2+} transients in Merkel cells. **a** TG (1 μM) increased resting fura-2 ratios (F_{340}/F_{380}) in Merkel cells bathed in Ringer's solution. This increase was reversed by the addition of 10 mM EGTA (N=49 cells). **b** Under control conditions, fura-2 ratios consistently increased upon repeated depolarization with 135-mM K^+ Ringer's solution (N=10 cells). Peak magnitudes were 86–88% of the previous depolarization. **c** The depolarization-induced increase in fura-2 ratios was depressed by 1 μM TG. Cells were continuously exposed to TG beginning 10 min before the second high K^+ challenge (N=17 cells). Data are representative of four independent experiments. *Error bars* denote SEM

cells, we used thapsigargin (TG), a specific blocker of the endoplasmic reticulum Ca^{2+} ATPase, to deplete intracellular Ca^{2+} stores. Application of 1 μM TG to dissociated Merkel cells bathed in Ringer's solution (2 mM Ca^{2+}) caused an increase in $[Ca^{2+}]_{in}$ (Fig. 3a), as observed by an increase in Fura-2 ratios (F_{340}:F_{380}) from the resting levels of 0.56± 0.01 to 0.74±0.01 (N=52 cells). The subsequent application of external EGTA reduced Ca^{2+} influx into cells and quickly caused a decrease in $[Ca^{2+}]_{in}$, to a level slightly below resting values. These results indicate that Merkel cells actively sequester Ca^{2+} in stores.

To determine whether Ca^{2+} release from stores contributes to Ca^{2+} signaling in Merkel cells, we examined how store depletion alters depolarization-induced Ca^{2+} transients, which are abolished by antagonists of P/Q and L-type Ca^{2+} channels [9]. In control conditions, repeated depolarization with high K^+ solution induced Ca^{2+} transients whose peak magnitudes were 86–88% that of the previous depolarization (Fig. 3b). By contrast, in the presence of 1 μM TG peak Ca^{2+} transients were reduced to 14% of control values (Fig. 3c). This remaining Ca^{2+} transient observed after internal stores were emptied likely reflects Ca^{2+} influx through voltage-activated Ca^{2+} channels. Because depolarization-induced Ca^{2+} transients are abolished by voltage-activated Ca^{2+} channel inhibitors [9] and are dramatically reduced by store depletion (Fig. 3c), these results together indicate that Ca^{2+} influx through voltage-activated Ca^{2+} channels triggers Ca^{2+} release from internal stores.

Merkel cells express voltage-activated K^+ and BK_{Ca} channels

Our previous gene-profiling studies indicated that Merkel cells express transcripts encoding multiple K^+ channel isoforms, including the β1 (KCNMB1) accessory subunit of BK_{Ca} channels [9]. Given that Merkel cells have robust Ca^{2+} transients, it is possible that currents from BK_{Ca} channels regulate the membrane potential of these cells. We therefore asked whether BK_{Ca} channels contribute to voltage-activated K^+ currents in Merkel cells.

To determine whether Merkel cells express BK_{Ca} channels, we used immunohistochemistry in skin cryosections. Merkel cells in touch domes and whisker follicles showed robust labeling by an antibody recognizing the pore-forming α subunit of BK_{Ca} channels (Fig. 4a,b). By contrast to the $Ca_V2.1$ staining, BK_{Ca} staining was diffuse on the plasma membrane of both whisker and touch-dome Merkel cells. To determine whether BK_{Ca} channel accessory β subunits are expressed in Merkel cells, we used reverse transcription and polymerase chain reaction to amplify products from cDNA derived from FACS-purified GFP^+ Merkel cells. Primers specific for the pore-forming α subunit gene, KCNMA1, and accessory subunits β2 (KCNMB2) and β4 (KCNMB4) yielded amplicons of the expected sizes (Fig. 4c). Primers specific for β1 (KCNMB1) amplified multiple splice variants, whose identities were verified by sequencing. By contrast, no detectable product was amplified from Merkel-cell cDNA using primers specific for β3 (KCNMB3).

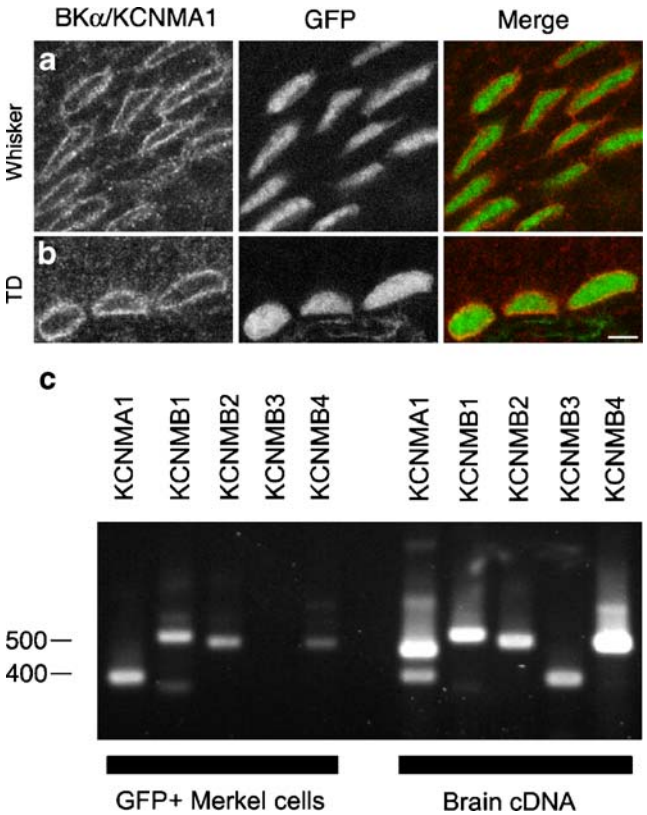

Fig. 4 Merkel cells express BKCa channels. **a** Immunoreactivity against the BK_{Ca} α subunit (KCNMA1) was detected in GFP^+ Merkel cells in skin cryosections of whisker follicles (**a**) and touch domes (**b**). *Right panels* show merged images of immunoreactivity (*left panels* and *red*) and GFP fluorescence (*middle panels* and *green*). *Scale bar* represent 10 μm for all panels. **c** PCR products were amplified from cDNA derived from FACS-purified, GFP^+ Merkel cells with primers specific for the indicated BK_{Ca} subunits. Brain cDNA served as a positive control template for all primer pairs. KCNMA1 and KCNMB1 primer pairs yielded multiple amplicons that encoded splice variants

In whole-cell recordings from dissociated Merkel cells, we found that BK_{Ca} channels carry the majority of the voltage-activated K^+ current. K^+ currents were recorded in response to voltage steps from −80 mV to +120 mV. Merkel cells had robust and complicated K^+ currents, whose kinetics and magnitude varied from cell to cell (Fig. 5a,e; N=32 cells). Approximately 60–70% of the current was blocked by 100 nM IBTX, a specific blocker of BK_{Ca} channels [24]. Most of the remaining IBTX-insensitive current was blocked by 6 mM external TEA, indicating that it was carried by delayed rectifier K^+ channels. The magnitude of this TEA-sensitive K^+ current varied between 60 and 200 pA at +90 mV with an average magnitude of 137±85 pA (N=8). The remaining TEA-insensitive current, which was found to be selective for Cl^- by ion substitution experiments, ranged between 20 and 100 pA, with an average magnitude at +60 mV of 64±23 pA (N=8).

To isolate BK_{Ca} currents from other K^+ currents, traces of IBTX-blocked currents were subtracted from whole-cell currents. The resulting IBTX-sensitive traces correspond to currents through BK_{Ca} channels (Fig. 5c,g). Cells were categorized based on whether the IBTX-sensitive currents had an inactivating component. For cells with an inactivating BK_{Ca} component (62%), peak currents at +90 mV ranged from 50 to 250 pA (mean±SEM=140±60 pA, or 17 pA/pF; N=10 cells). Inactivating BK_{Ca} currents began to turn on at −40 mV (Fig. 5d), whereas the non-inactivating component of the BK_{Ca} current were observable in the range of 0 to +20 mV (Fig. 5h). For cells that lacked a detectable inactivating BK_{Ca} component (38%), the magnitude of the current varied between 300 and 1,000 pA, with an average peak at +90 mV of 585±20 pA, or 10±1.1 pA/pF (N=9). The variability of BK_{Ca} currents is consistent with the expression of multiple β subunits, which alter the kinetics and voltage-sensitivity of these channels [25–27].

To characterize the Ca^{2+} sensitivity of BK_{Ca} channels in Merkel cells, we pulled inside-out patches from Merkel cells and measured the activity of the channels as the $[Ca^{2+}]$ in the bath was altered (Fig. 6a). We found that channel activity was augmented by increasing free $[Ca^{2+}]$ from subnanomolar $[Ca^{2+}]_{free}$ to 10 μM $[Ca^{2+}]_{free}$ (Fig. 6b; N=5

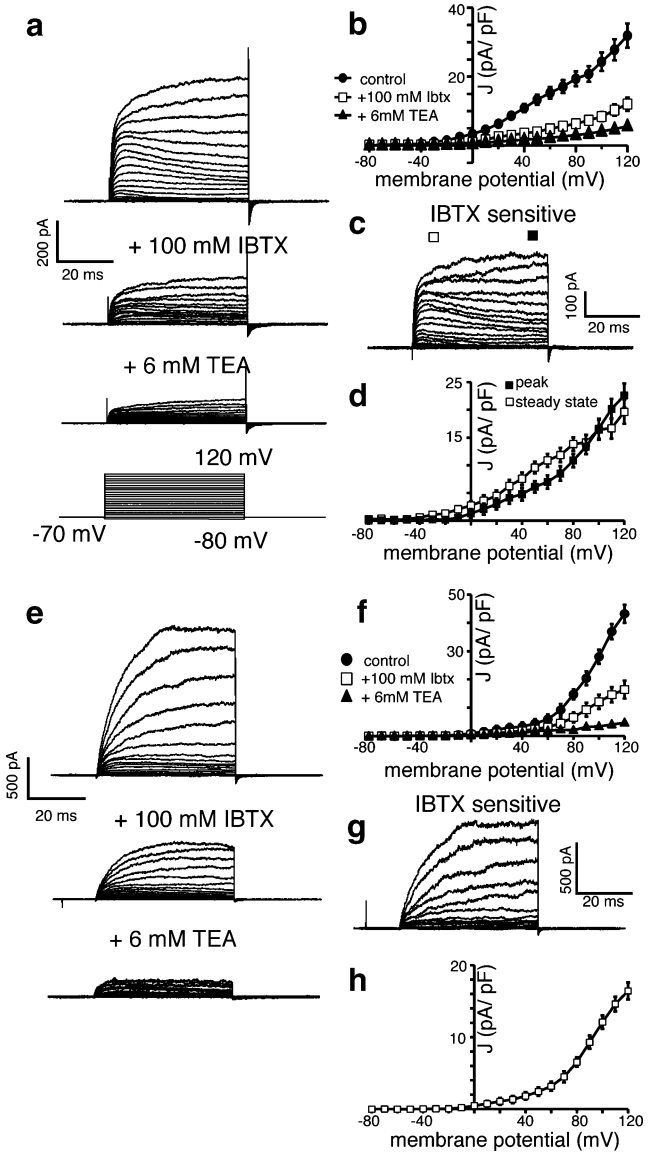

Fig. 5 Merkel cells have BK_{Ca} and voltage-activated K^+ currents. **a** Representative whole-cell K^+ currents with an inactivating component (*top traces*) recorded from a touch-dome Merkel cell during a series of depolarizing steps (*bottom traces*). A large fraction of the current, including the inactivating component was blocked by 100 nM IBTX (*second set of traces*). The remaining current was further blocked by 6 mM TEA (*third set of traces*). **b** Peak K^+ current densities during the depolarizing step plotted as a function of membrane potential for the currents shown (**a**). *Error bars* denote SEM (N=10 responses). **c** IBTX-sensitive currents were isolated from the traces in **a** by subtracting IBTX-sensitive traces from the total K^+ current. This cell displayed both inactivating and non-inactivating components that were blocked by IBTX. **d** Peak current densities from the first 20 ms (*open squares*) and steady-state currents from the last 20 ms of the depolarizing pulse (*filled squares*) were plotted as a function of voltage (N=10 responses). **e** Representative whole-cell K^+ currents lacking an inactivating component (*top traces*) recorded from a touch-dome Merkel cell under the same protocol and pharmacological conditions shown in **a**. **f** Peak K^+ current densities during the depolarizing step plotted as a function of membrane potential for the currents shown (**e**). *Error bars* denote SEM (N=9 responses). **g** Isolated IBTX-sensitive currents from the traces in **e**. **h** Steady-state current densities from the last 20 ms of the depolarizing pulse (*filled squares*) were plotted as a function of voltage (N=9 responses)

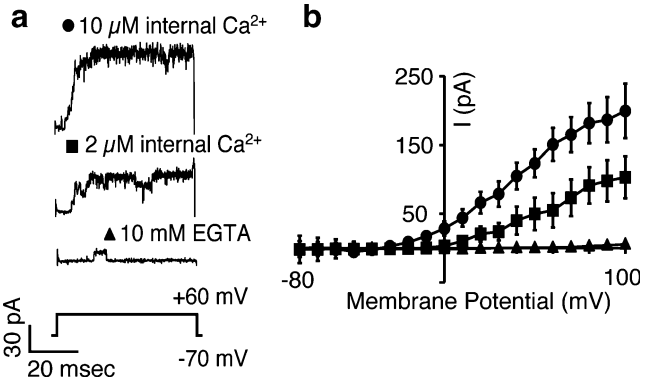

Fig. 6 K^+ currents in Merkel cells respond to changes in internal Ca^{2+}. **a** Currents from a representative inside-out patch pulled from a Merkel cell in response to a voltage step to +60 mV. The $[Ca^{2+}]$ of the internal solutions (bath) was set to 10 μM (*circles*), 2 μM (*squares*) and subnanomolar levels with 10 mM EGTA (*triangles*). **b** Average current from five patches for the three $[Ca^{2+}]$. *Error bars* denote SEM

experiments). These data indicate that BK_{Ca} channels in Merkel cells are activated by micromolar changes in $[Ca^{2+}]_{in}$.

BK_{Ca} channels are modulated primarily by Ca^{2+} influx across the plasma membrane

BK_{Ca} channel activity can be coupled either to Ca^{2+} store release, to Ca^{2+} influx through voltage-activated Ca^{2+} channels or to both. To distinguish between these possibilities in Merkel cells, we measured voltage-activated K^+ currents under various Ca^{2+} conditions. First, we asked whether Merkel cells' BK_{Ca} channels are modulated by global changes in cytoplasmic Ca^{2+}. To do so, we measured the activity of the voltage-activated K^+ currents in the presence of 1 μM TG and 2 mM extracellular Ca^{2+}, which increased average cytoplasmic $[Ca^{2+}]$ by preventing the refilling of stores (Fig. 3a). Under these conditions, we saw a small (18±3%; N=4 cells) increase in the magnitude of voltage-activated K^+ currents in the presence of 1 μM TG (Fig. 7a; open squares). In the presence of 100 nM IBTX, we saw no change in the voltage-activated K^+ current, indicating that the increased current is due to BK_{Ca} activity (Fig. 7b, open triangles; N=3 cells).

We next measured the voltage-activated K^+ current in the presence of external EGTA to eliminate Ca^{2+} influx through voltage-activated Ca^{2+} channels and subsequent CICR. Under these conditions, voltage-activated K^+ currents were dramatically reduced by 80±2% (Fig. 7c, open diamonds; N=7 cells). As a control (Fig. 7b; N=3 cells), we reduced the extracellular $[Ca^{2+}]$ (filled diamonds) or depleted Ca^{2+} stores with 1 μM TG in the presence of IBTX (open triangles). These treatments yielded voltage-activated currents that were indistinguishable from IBTX alone (open diamonds), indicating that BK_{Ca} channels are solely responsible for the current that is sensitive to the

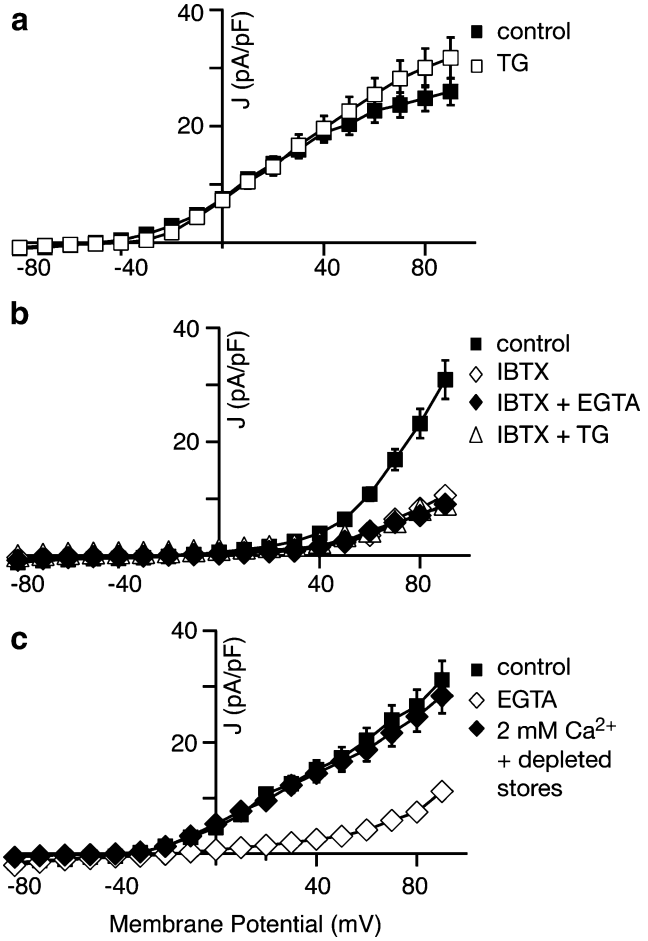

Fig. 7 BK_{Ca} currents in Merkel cells are coupled to voltage-activated Ca^{2+} channels rather than CICR. **a** Peak current densities as a function of voltage before (*filled squares*) and after (*open squares*) the addition of 1 μM TG to prevent Ca^{2+} uptake into stores (N=4 cells). **b** Peak current densities from another set of cells plotted as a function of voltage before (*filled squares*) and after (*open diamonds*) the addition of 100 nM IBTX; 100 nM IBTX and 10 mM EGTA (*filled diamonds*); and 100 nM IBTX and 1 μM TG (*open triangles*). All traces with IBTX superimpose (N=3 cells). **c** Peak current from a set of cells plotted as a function of voltage before (*filled squares*) and after (*open diamonds*) bath perfusion of 10 mM EGTA and 1 μM TG. After depleting stores (10 min in EGTA and TG with repeated depolarizations), extracellular Ca^{2+} was restored to 2 mM and the current densities were plotted as a function of voltage (*filled diamonds*; N=4 cells). All *error bars* denote SEM

changes in extracellular $[Ca^{2+}]$ and Ca^{2+}-store release. These results indicate that BK_{Ca} channels are tightly coupled to either Ca^{2+} influx at the plasma membrane or to CICR.

To uncouple store release from Ca^{2+} influx at the plasma membrane, we depleted stores with 1 μM TG in the presence of external EGTA for 10 min (Fig. 7c; filled diamonds, N=4 cells). Our live-cell Ca^{2+}-imaging experiments demonstrated that stores are depleted under these conditions (Fig. 3a,c, and data not shown). With internal stores depleted, we measured voltage-activated K^+ currents in the presence of 2 mM external $[Ca^{2+}]$ to allow Ca^{2+} influx through voltage-activated Ca^{2+} channels and found that BK_{Ca} currents were only slightly lower than the current magnitude in control conditions (91±2% of control; N=4 cells). Strikingly, the store-depleted BK_{Ca} current (Fig. 7c; filled diamonds) was threefold larger than the current in the presence of external EGTA (Fig. 7c; open diamonds), which eliminates both Ca^{2+} influx and store release. Together, these results demonstrate that BK_{Ca} channel activity is predominantly coupled to Ca^{2+} influx through voltage-activated Ca^{2+} channels and only modestly regulated by CICR.

Voltage-activated K^+ channels regulate Ca^{2+} signaling in Merkel cells

We next asked whether voltage-activated K^+ channels alter the time course and magnitude of Ca^{2+} signals in Merkel cells, as they do in neurons. Because Merkel cells are proposed to function as mechanoreceptor cells [4], we used a mechanical stimulus, hypotonic-induced cell swelling, to excite dissociated Merkel cells [15, 16, 28].

Merkel cells were bathed in a 20% hypotonic extracellular solution either in the presence or absence of TEA to block BK_{Ca} and delayed-rectifying voltage-activated K^+ channels. In Merkel cells stimulated with 20% hypotonic solutions, we observed increases in $[Ca^{2+}]_{in}$ that decayed slowly during sustained hypotonic stimulation (Fig. 8a and [16]). The addition of external TEA to block K^+ channels transformed these smooth $[Ca^{2+}]_{in}$ increases into Ca^{2+} transients with complex time courses that varied among individual Merkel cells (Fig. 8a). Peak fura-2 ratios were significantly increased in the presence of TEA (Fig. 8b; mean±SEM: control, 1.18±0.10; TEA, 1.85±0.13; N=25 cells). TEA also significantly increased the rate of onset of swelling-evoked Ca^{2+} transients (Fig. 8c; mean±SEM: control, 20.9±2.1 s; TEA, 12.6±3.2 s; N=21 cells). Surprisingly, we found that the decay time during the hypotonic challenge, defined as the elapsed time for a 20% drop from peak response, was significantly shortened in the presence of TEA (Fig. 8d; mean±SEM, control: 13.2± 2.6 s; TEA: 5.2±1.7 s; N=8 cells). These results indicate that voltage-activated K^+ channels limit the extent and prolong the duration of mechanically evoked Ca^{2+} transients in Merkel cells.

To ask specifically if BK_{Ca} channels modulate Ca^{2+} transients in Merkel cells, we incubated Merkel cells in 100 nM IBTX for ≥10 min. We found that this treatment increased the resting fura-2 ratios by 10.5±0.4%, (N=119 cells). This suggests that BK_{Ca} channels regulate Ca^{2+} influx in Merkel cells by contributing to the resting membrane potential; however, this resting Ca^{2+} increase confounded the interpretation of Ca^{2+} transients in Merkel cells.

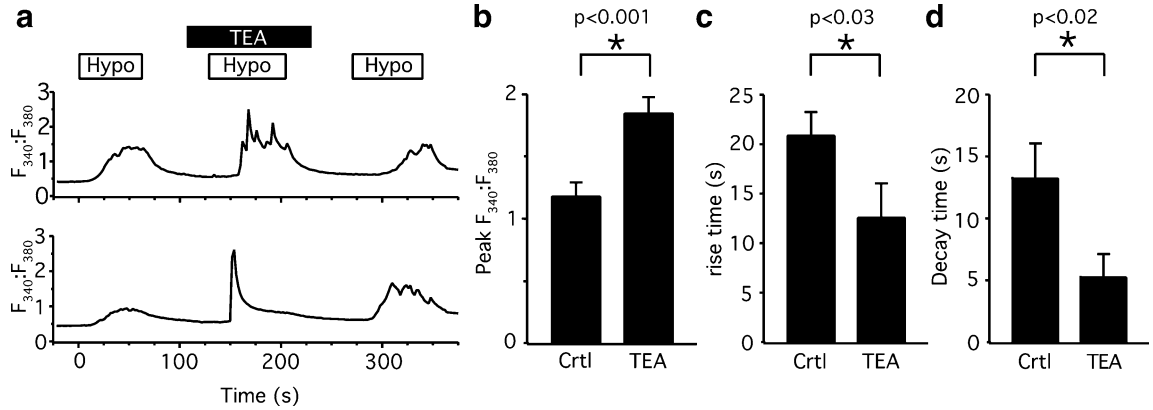

Fig. 8 K^+ channels shape hypotonic-evoked Ca^{2+} transients in Merkel cells. **a** Increases in Fura-2 fluorescent ratios (F_{340}:F_{380}) were elicited by bathing cells in a 20% hypotonic solution (232 mmol·kg^{-1}) in the absence or presence of 30 mM TEA. Responses of two representative cells are shown. **b** In the presence of TEA, the hypotonic-induced fluorescence change was significantly greater than in control conditions (N=25 cells). **c–d** Both the rise time and relaxation time of hypotonic-evoked fluorescence increase were significantly faster than in control conditions. Rise time was defined as the elapsed time between 10% and 90% of the peak value (N=21 cells). Relaxation time was defined as the elapsed time between 100% and 80% of the peak value (N=8 cells). Data are derived from two independent experiments. *Error bars* represent SEM. *Asterisks* indicate statistically different populations at the significance levels noted (paired Wilcoxon signed-rank test)

Discussion

Previous studies in semi-intact preparations have implicated Ca^{2+} signaling in touch-evoked responses of Merkel cell–neurite complexes [5–7]. Here, we have provided direct evidence that the Merkel cell's voltage-activated Ca^{2+} channels generate Ca^{2+} transients that are amplified by CICR. Furthermore, we have described the activity of voltage-activated K^+ channels and BK_{Ca} channels and have shown that the latter are coupled to Ca^{2+} influx at the plasma membrane. Finally, we have demonstrated that voltage-activated K^+ currents both limit the amplitude and prolong the time course of Ca^{2+} transients induced by a mechanical stimulus. Collectively, these results uncover a network of ion channels and Ca^{2+} signaling mechanisms that are active in Merkel cells and that may modulate the transduction of mechanical stimuli. In hair cells and photoreceptors, these mechanisms regulate sensory signaling by either controlling frequency tuning or synaptic function [29–32].

By immunohistochemistry, we demonstrated that Merkel cells in the intact skin express the P/Q-type isoform $Ca_V2.1$. Moreover, we recorded voltage-activated Ca^{2+} channel currents in mouse Merkel cells purified from whisker follicles and touch domes. Our results extend previous studies indicating that Merkel cells express transcripts encoding N-, P/Q-, and L-type Ca^{2+} channels [9] and that rat footpad Merkel cells have voltage-activated Ca^{2+} currents [8]. The voltage-activated Ca^{2+} channel currents that we report in this study have similar activation ranges, kinetics, and magnitudes as those described in rat footpad Merkel cells [8]. As in footpad Merkel cells, we did not observe voltage-activated Na^+ conductances in mouse whisker-follicle and touch-dome Merkel cells. Although Yamashita et al. reported "long-lasting action potentials" in Ba^{2+} external solutions, we did not observe spiking activity in current-clamp recordings (R. P. and E. A. L., data not shown).

A key function of voltage-activated Ca^{2+} channels in neuroendocrine cells is to trigger synaptic vesicle release [33, 34], and we hypothesize that they do so in Merkel cells. Along with L-type and P/Q-type Ca^{2+} channels, Merkel cells have been shown to express the same vesicle release machinery as neurons and sensory cells [9]. Furthermore, there is mounting evidence from recordings of SAI receptors in semi-intact preparations that chemical synaptic transmission plays a role in touch [35–37]. Intriguingly, our results indicate that $Ca_V2.1$ protein is localized to the microvilli of Merkel cells, which indicates that these channels may serve additional signaling roles.

We also demonstrated that Merkel cells employ CICR to generate robust $[Ca^{2+}]_{in}$ transients downstream of voltage-activated Ca^{2+} channels. These results agree with prior evidence that Merkel cells express IP_3Rs [10] as well as semi-intact recordings that indicate SAI responses involve ryanodine-receptor activation [7]. If Merkel cells, like hair cells [38] and mechanosensitive neurons [39], respond to mechanical stimuli by activation of transduction channels, CICR could be a mechanism enabling small stimuli to invoke robust synaptic vesicle release. This mechanism has recently been shown to amplify synaptic transmission in sensory cells, including hair cells, rod photoreceptors, and amacrine cells [40–42]. The remarkably low thresholds of SAI responses [2] suggest that an amplification process could play a role in touch reception.

Along with voltage-activated Ca^{2+} channels, we have shown that Merkel cells have complex voltage-activated K^+

currents. Merkel cells from the rat footpad have currents that activate over a similar voltage range and display a similar TEA sensitivity to the total K^+ current we recorded; however, the observed inactivation timescales differ [8]. Here, we show that the majority of this K^+ current is carried by IBTX-sensitive BK_{Ca} channels, which are strongly modulated by Ca^{2+} entry through voltage-activated Ca^{2+} channels rather than by Ca^{2+} release from stores. Consistent with this finding, we demonstrated that non-inactivating Merkel-cell BK_{Ca} channels activate over a voltage range that encompasses the potentials that open voltage-activated Ca^{2+} channels. We found that BK_{Ca} currents have complex kinetic properties and activation ranges that varied among Merkel cells. To harvest sufficient cell numbers for recordings, we typically pooled touch domes and whisker follicles for Merkel-cell isolation; therefore, it is possible that some of the observed variability reflects differences in Merkel cells from these two tissues. This cannot account for all of the variability, however, because we observed both inactivating and non-inactivating BK_{Ca} currents in touch-dome Merkel cells (e.g., Fig. 5a,e). These data highlight the functional diversity of Merkel cells, which is consistent with the observation that distinct populations of Merkel cells have different neurotrophic dependencies [43]. The physiological consequences of this functional and developmental diversity merits future investigation.

Why do the properties of the BK_{Ca} current vary from cell to cell? Such complexity of BK_{Ca} current has been observed in hair cells [44, 45] and chromaffin cells [46]. In these cell types, different BK_{Ca} properties are due to the differential expression of accessory β subunits [25–27] and α-subunit splice variants [47–49]. The IBTX-sensitive inactivating currents that we described, as well as the differing activation ranges of the sustained and transient components, indicate that Merkel cells express multiple accessory β subunits. Consistent with this notion, we detected the expression of three accessory β subunits (Fig. 4), and the expression of β1 has been previously reported in Merkel cells [9]. Because mechanoreceptors are proposed to be tuned to a whisker's resonant frequency [50], it is possible that this differential expression of BK_{Ca} channels in Merkel cells contribute to tuning at the cellular level, as they do in chick auditory hair cells [48, 51, 52]. In addition to tuning sensory receptor cells, BK_{Ca} channels regulate neurotransmitter release in sensory cells [29, 53] and excitability in a variety of systems [54–57]. Moreover, BK_{Ca} provides critical feedback regulation of contractility of mechanically sensitive smooth muscle [58–61]. Our demonstration that blocking voltage-activated K^+ and BK_{Ca} currents dramatically altered the extent and time course of Ca^{2+} transients in Merkel cells indicates that these channels regulate Merkel-cell signaling.

To determine how voltage-activated K^+ channels modulate mechanically evoked signaling in Merkel cells, we used hypotonic-evoked cell swelling, which is an established experimental paradigm for mechanically stimulating cells in vitro and in vivo. Hypotonic stimuli have been shown to excite mechanosensory cells, including outer hair cells and somatosensory neurons [62, 63]. Moreover, candidate mechanotransduction channels are osmosensitive when expressed in heterologous systems [64, 65]. Finally, hypotonic stimuli have been shown to excite Merkel cells [15, 16, 28].

Because voltage-activated K^+ channels generally limit excitability in neuroendocrine cells, it seems paradoxical that blocking BK_{Ca} and other voltage-activated K^+ channels shortens hypotonic-evoked Ca^{2+} transients in Merkel cells. Such counterintuitive effects of BK_{Ca} blockers have been reported in other cell types [29, 66–68]. The Ca^{2+} transients we observe in Merkel cells reflects a balance between Ca^{2+} influx, release from stores, and sequestration by buffering and extrusion [69]. These processes are all modulated by Ca^{2+} [69] and are therefore potential sites of regulation by BK_{Ca} and voltage-activated K^+ channels. For example, by limiting membrane depolarization and $[Ca^{2+}]_{in}$, K^+ channels may delay inactivation of voltage-activated Ca^{2+} channels thereby prolonging the Ca^{2+} transient. Furthermore, BK_{Ca} and Cl^- channels have been found to link to intracellular Ca^{2+} dynamics during regulatory volume decrease after hypotonic stimulation [70, 71].

In summary, we have shown that membrane depolarization in Merkel cells activates a Ca^{2+} signaling cascade that includes voltage-activated Ca^{2+} channels, CICR, and BK_{Ca} channels. Although the role of Merkel cells in mechanotransduction is still an open question, our characterization of these cellular signaling mechanisms lays the necessary foundation for future experiments to determine the physiological role of activated Merkel cells in touch.

Acknowledgements We thank Dr. Diana Bautista and Ms. Carla Webster for experimental advice. Drs. Peter Gillespie and Richard Aldrich provided comments on the manuscript. This work, which was begun at UC San Francisco, was supported by the Sandler Program in Basic Sciences and the National Institutes of Health (National Institute of Arthritis and Musculoskeletal and Skin Diseases grant AR051219).

References

1. Johnson KO (2001) The roles and functions of cutaneous mechanoreceptors. Curr Opin Neurobiol 11:455–461
2. Iggo A, Muir AR (1969) The structure and function of a slowly adapting touch corpuscle in hairy skin. J Physiol 200:763–796
3. Woodbury CJ, Koerber HR (2007) Central and peripheral anatomy of slowly adapting type I low-threshold mechanoreceptors

innervating trunk skin of neonatal mice. J Comp Neurol 505:547–561
4. Halata Z, Grim M, Bauman KI (2003) Friedrich Sigmund Merkel and his "Merkel cell", morphology, development, and physiology: review and new results. Anat Rec 271A:225–239
5. Yamashita Y, Ogawa H, Taniguchi K (1986) Differential effects of manganese and magnesium on two types of slowly adapting cutaneous mechanoreceptor afferent units in frogs. Pflugers Arch 406:218–224
6. Pacitti EG, Findlater GS (1988) Calcium channel blockers and Merkel cells. Prog Brain Res 74:37–42
7. Senok SS, Baumann KI (1997) Functional evidence for calcium-induced calcium release in isolated rat vibrissal Merkel cell mechanoreceptors. J Physiol 500(Pt 1):29–37
8. Yamashita Y, Akaike N, Wakamori M, Ikeda I, Ogawa H (1992) Voltage-dependent currents in isolated single Merkel cells of rats. J Physiol 450:143–162
9. Haeberle H, Fujiwara M, Chuang J, Medina MM, Panditrao M, Bechstedt S, Howard J, Lumpkin EA (2004) Molecular profiling reveals synaptic release machinery in Merkel cells. Proc Natl Acad Sci U S A 101:14503–14508
10. Tachibana T, Endoh M, Kumakami R, Nawa T (2003) Immunohistochemical expressions of mGluR5, P2Y2 receptor, PLC-beta1, and IP3R-I and -II in Merkel cells in rat sinus hair follicles. Histochem Cell Biol 120:13–21
11. Sekerkova G, Zheng L, Loomis PA, Changyaleket B, Whitlon DS, Mugnaini E, Bartles JR (2004) Espins are multifunctional actin cytoskeletal regulatory proteins in the microvilli of chemosensory and mechanosensory cells. J Neurosci 24:5445–5456
12. Hansel C, Linden DJ, D'Angelo E (2001) Beyond parallel fiber LTD: the diversity of synaptic and non-synaptic plasticity in the cerebellum. Nat Neurosci 4:467–475
13. Newman EA (2001) Propagation of intercellular calcium waves in retinal astrocytes and Muller cells. J Neurosci 21:2215–2223
14. Chan E, Yung WH, Baumann KI (1996) Cytoplasmic Ca^{2+} concentrations in intact Merkel cells of an isolated, functioning rat sinus hair preparation. Exp Brain Res 108:357–366
15. Tazaki M, Suzuki T (1998) Calcium inflow of hamster Merkel cells in response to hyposmotic stimulation indicate a stretch activated ion channel. Neurosci Lett 243:69–72
16. Haeberle H, Bryan LA, Vadakkan TJ, Dickinson ME, Lumpkin EA (2008) Swelling-activated Ca^{2+} channels trigger Ca^{2+} signals in Merkel cells. PLoS ONE 3(3):e1750. DOI 10.1371/journal.pone.0001750
17. Lumpkin EA, Collisson T, Parab P, Omer-Abdalla A, Haeberle H, Chen P, Doetzlhofer A, White P, Groves A, Segil N, Johnson JE (2003) Math1-driven GFP expression in the developing nervous system of transgenic mice. Gene Expr Patterns 3:389–395
18. Koltzenburg M, Stucky CL, Lewin GR (1997) Receptive properties of mouse sensory neurons innervating hairy skin. J Neurophysiol 78:1841–1850
19. Rozen S, Skaletsky HJ (2000) Primer3 on the WWW for general users and for biologist programmers. In: Krawetz S, Misener S (eds) Bioinformatics methods and protocols: methods in molecular biology. Humana, Totowa, NJ, pp 365–386
20. Falke LC, Gillis KD, Pressel DM, Misler S (1989) 'Perforated patch recording' allows long-term monitoring of metabolite-induced electrical activity and voltage-dependent Ca2+ currents in pancreatic islet B cells. FEBS Lett 251:167–172
21. Neher E (1992) Correction for liquid junction potentials in patch clamp experiments. Methods Enzymol 207:123–131
22. Hille B (2001) Ion channels of excitable membranes, 3rd edn. Sinauer, Sunderland, MA
23. Fox AP, Nowycky MC, Tsien RW (1987) Kinetic and pharmacological properties distinguishing three types of calcium currents in chick sensory neurones. J Physiol 394:149–172
24. Kunze WA, Bornstein JC, Furness JB, Hendriks R, Stephenson DS (1994) Charybdotoxin and iberiotoxin but not apamin abolish the slow after-hyperpolarization in myenteric plexus neurons. Pflugers Arch 428:300–306
25. Ding JP, Li ZW, Lingle CJ (1998) Inactivating BK channels in rat chromaffin cells may arise from heteromultimeric assembly of distinct inactivation-competent and noninactivating subunits. Biophys J 74:268–289
26. Ramanathan K, Michael TH, Fuchs PA (2000) beta subunits modulate alternatively spliced, large conductance, calcium-activated potassium channels of avian hair cells. J Neurosci 20:1675–1684
27. Hafidi A, Beurg M, Dulon D (2005) Localization and developmental expression of BK channels in mammalian cochlear hair cells. Neuroscience 130:475–484
28. Baumann KI, Senok SS, Chan E, Yung WH (2000) Calcium influx and calcium-induced calcium release in mechanically stimulated Merkel cells of rat sinus hair type I mechanoreceptors. In: Suzuki H, Ono T (eds) Merkel cells, Merkel cell carcinoma and neurobiology of the skin. Elsevier, Amsterdam, pp 73–81
29. Xu JW, Slaughter MM (2005) Large-conductance calcium-activated potassium channels facilitate transmitter release in salamander rod synapse. J Neurosci 25:7660–7668
30. Lewis RS, Hudspeth AJ (1983) Voltage- and ion-dependent conductances in solitary vertebrate hair cells. Nature 304:538–541
31. Corey DP, Dubinsky JM, Schwartz EA (1984) The calcium current in inner segments of rods from the salamander (Ambystoma tigrinum) retina. J Physiol 354:557–575
32. Fuchs PA, Nagai T, Evans MG (1988) Electrical tuning in hair cells isolated from the chick cochlea. J Neurosci 8:2460–2467
33. Hirning LD, Fox AP, McCleskey EW, Olivera BM, Thayer SA, Miller RJ, Tsien RW (1988) Dominant role of N-type Ca2+ channels in evoked release of norepinephrine from sympathetic neurons. Science 239:57–61
34. Reid CA, Bekkers JM, Clements JD (2003) Presynaptic Ca2+ channels: a functional patchwork. Trends Neurosci 26:683–687
35. Fagan BM, Cahusac PM (2001) Evidence for glutamate receptor mediated transmission at mechanoreceptors in the skin. Neuroreport 12:341–347
36. He L, Tuckett RP, English KB (2003) 5-HT2 and 3 receptor antagonists suppress the response of rat type I slowly adapting mechanoreceptor: an in vitro study. Brain Res 969:230–236
37. Cahusac PM, Senok SS, Hitchcock IS, Genever PG, Baumann KI (2005) Are unconventional NMDA receptors involved in slowly adapting type I mechanoreceptor responses. Neuroscience 133:763–773
38. Gillespie PG, Walker RG (2001) Molecular basis of mechanosensory transduction. Nature 413:194–202
39. Drew LJ, Wood JN, Cesare P (2002) Distinct mechanosensitive properties of capsaicin-sensitive and -insensitive sensory neurons. J Neurosci 22:RC228
40. Lelli A, Perin P, Martini M, Ciubotaru CD, Prigioni I, Valli P, Rossi ML, Mammano F (2003) Presynaptic calcium stores modulate afferent release in vestibular hair cells. J Neurosci 23:6894–6903
41. Chavez AE, Singer JH, Diamond JS (2006) Fast neurotransmitter release triggered by Ca influx through AMPA-type glutamate receptors. Nature 443:705–708
42. Suryanarayanan A, Slaughter MM (2006) Synaptic transmission mediated by internal calcium stores in rod photoreceptors. J Neurosci 26:1759–1766
43. Cronk KM, Wilkinson GA, Grimes R, Wheeler EF, Jhaveri S, Fundin BT, Silos-Santiago I, Tessarollo L, Reichardt LF, Rice FL (2002) Diverse dependencies of developing Merkel innervation on the trkA and both full-length and truncated isoforms of trkC. Development 129:3739–3750

44. Art JJ, Fettiplace R (1987) Variation of membrane properties in hair cells isolated from the turtle cochlea. J Physiol 385:207–242
45. Pyott SJ, Glowatzki E, Trimmer JS, Aldrich RW (2004) Extrasynaptic localization of inactivating calcium-activated potassium channels in mouse inner hair cells. J Neurosci 24:9469–9474
46. Solaro CR, Prakriya M, Ding JP, Lingle CJ (1995) Inactivating and noninactivating Ca(2+)- and voltage-dependent K+ current in rat adrenal chromaffin cells. J Neurosci 15:6110–6123
47. Langer P, Grunder S, Rusch A (2003) Expression of Ca2+-activated BK channel mRNA and its splice variants in the rat cochlea. J Comp Neurol 455:198–209
48. Rosenblatt KP, Sun ZP, Heller S, Hudspeth AJ (1997) Distribution of Ca2+-activated K+ channel isoforms along the tonotopic gradient of the chicken's cochlea. Neuron 19:1061–1075
49. Navaratnam DS, Bell TJ, Tu TD, Cohen EL, Oberholtzer JC (1997) Differential distribution of Ca2+-activated K+ channel splice variants among hair cells along the tonotopic axis of the chick cochlea. Neuron 19:1077–1085
50. Andermann ML, Ritt J, Neimark MA, Moore CI (2004) Neural correlates of vibrissa resonance; band-pass and somatotopic representation of high-frequency stimuli. Neuron 42:451–463
51. Fuchs PA, Evans MG (1990) Potassium currents in hair cells isolated from the cochlea of the chick. J Physiol 429:529–551
52. Ramanathan K, Michael TH, Jiang GJ, Hiel H, Fuchs PA (1999) A molecular mechanism for electrical tuning of cochlear hair cells. Science 283:215–217
53. Beurg M, Hafidi A, Skinner LJ, Ruel J, Nouvian R, Henaff M, Puel JL, Aran JM, Dulon D (2005) Ryanodine receptors and BK channels act as a presynaptic depressor of neurotransmission in cochlear inner hair cells. Eur J Neurosci 22:1109–1119
54. Wang ZW, Saifee O, Nonet ML, Salkoff L (2001) SLO-1 potassium channels control quantal content of neurotransmitter release at the C. elegans neuromuscular junction. Neuron 32:867–881
55. Greffrath W, Magerl W, Disque-Kaiser U, Martin E, Reuss S, Boehmer G (2004) Contribution of Ca2+-activated K+ channels to hyperpolarizing after-potentials and discharge pattern in rat supraoptic neurones. J Neuroendocrinol 16:577–588
56. Sausbier M, Hu H, Arntz C, Feil S, Kamm S, Adelsberger H, Sausbier U, Sailer CA, Feil R, Hofmann F, Korth M, Shipston MJ, Knaus HG, Wolfer DP, Pedroarena CM, Storm JF, Ruth P (2004) Cerebellar ataxia and Purkinje cell dysfunction caused by Ca2+-activated K+ channel deficiency. Proc Natl Acad Sci U S A 101:9474–9478
57. Raffaelli G, Saviane C, Mohajerani MH, Pedarzani P, Cherubini E (2004) BK potassium channels control transmitter release at CA3-CA3 synapses in the rat hippocampus. J Physiol 557:147–157
58. Petkov GV, Bonev AD, Heppner TJ, Brenner R, Aldrich RW, Nelson MT (2001) Beta1-subunit of the Ca2+-activated K+ channel regulates contractile activity of mouse urinary bladder smooth muscle. J Physiol 537:443–452
59. Werner ME, Zvara P, Meredith AL, Aldrich RW, Nelson MT (2005) Erectile dysfunction in mice lacking the large-conductance calcium-activated potassium (BK) channel. J Physiol 567:545–556
60. Thorneloe KS, Meredith AL, Knorn AM, Aldrich RW, Nelson MT (2005) Urodynamic properties and neurotransmitter dependence of urinary bladder contractility in the BK channel deletion model of overactive bladder. Am J Physiol Renal Physiol 289:F604–F610
61. Meredith AL, Thorneloe KS, Werner ME, Nelson MT, Aldrich RW (2004) Overactive bladder and incontinence in the absence of the BK large conductance Ca2+-activated K+ channel. J Biol Chem 279:36746–36752
62. Harada N, Ernst A, Zenner HP (1994) Intracellular calcium changes by hyposmotic activation of cochlear outer hair cells in the guinea pig. Acta Otolaryngol 114:510–515
63. Alessandri-Haber N, Yeh JJ, Boyd AE, Parada CA, Chen X, Reichling DB, Levine JD (2003) Hypotonicity induces TRPV4-mediated nociception in rat. Neuron 39:497–511
64. Kim J, Chung YD, Park DY, Choi S, Shin DW, Soh H, Lee HW, Son W, Yim J, Park CS, Kernan MJ, Kim C (2003) A TRPV family ion channel required for hearing in Drosophila. Nature 424:81–84
65. Gong Z, Son W, Chung YD, Kim J, Shin DW, McClung CA, Lee Y, Lee HW, Chang DJ, Kaang BK, Cho H, Oh U, Hirsh J, Kernan MJ, Kim C (2004) Two interdependent TRPV channel subunits, inactive and Nanchung, mediate hearing in Drosophila. J Neurosci 24:9059–9066
66. Pattillo JM, Yazejian B, DiGregorio DA, Vergara JL, Grinnell AD, Meriney SD (2001) Contribution of presynaptic calcium-activated potassium currents to transmitter release regulation in cultured Xenopus nerve-muscle synapses. Neuroscience 102:229–240
67. Skinner LJ, Enee V, Beurg M, Jung HH, Ryan AF, Hafidi A, Aran JM, Dulon D (2003) Contribution of BK Ca2+-activated K+ channels to auditory neurotransmission in the Guinea pig cochlea. J Neurophysiol 90:320–332
68. Warbington L, Hillman T, Adams C, Stern M (1996) Reduced transmitter release conferred by mutations in the slowpoke-encoded Ca2(+)-activated K+ channel gene of Drosophila. Invert Neurosci 2:51–60
69. Berridge MJ, Bootman MD, Roderick HL (2003) Calcium signalling: dynamics, homeostasis and remodelling. Nat Rev Mol Cell Biol 4:517–529
70. Weskamp M, Seidl W, Grissmer S (2000) Characterization of the increase in [Ca(2+)](i) during hypotonic shock and the involvement of Ca(2+)-activated K(+) channels in the regulatory volume decrease in human osteoblast-like cells. J Membr Biol 178:11–20
71. Jakab M, Ritter M (2006) Cell volume regulatory ion transport in the regulation of cell migration. Contrib Nephrol 152:161–180